Articles

Structure and Spectra of 4,5-μ-Tetracarbonyliron-hexaborane(10), $Fe(CO)_4B_6H_{10}$, and Its Conjugate Base, $[Fe(CO)_4B_6H_9]^-$

Dileep K. Srivastava, Nigam P. Rath,[†] and Lawrence Barton*

Department of Chemistry, University of Missouri—St. Louis, St. Louis, Missouri 63121

James D. Ragaini, Orin Hollander, Robert Godfroid, and Sheldon G. Shore

Department of Chemistry, The Ohio State University, Columbus, Ohio 43210

Received November 23, 1992

The chemistry of $B_6H_{10}Fe(CO)_4$ (I) and its conjugate base $[B_6H_9Fe(CO)_4]^-$ (II) has been extended. ^{11}B and ^1H NMR spectra and the crystal and molecular structure of I are reported. I crystallizes in the orthorhombic space group *Pbca*, with $a = 11.441(3)$ Å, $b = 11.696(4)$ Å, $c = 16.396(3)$ Å, and $Z = 8$. The crystal structure determination of this air-sensitive species indicates that the cage geometry is not substantially different from that of the parent borane. The position of the Fe atom is well below the basal B_5 plane, the dihedral angle being 55.7°. The angles around the Fe atom suggest trigonal-bipyramidal geometry with the axial Fe–C bond diverging from linearity by ca. 6°. I is readily deprotonated with KH to afford the conjugate base $[B_6H_9Fe(CO)_4]^-$ (II). Variable-temperature NMR spectra for II indicate complex dynamic processes, and the data are interpreted in terms of fluxional motion of the bridging H atoms, which is quenched at ca. −130 °C, and also of the borane cage relative to the $Fe(CO)_4$ moiety, which is quenched at ca. −10 °C. Two processes are identifed for the former: complete scrambling of the three bridging H atoms among the four available sites above −50 °C and a process that is partially quenched in which only one H atom moves above −100 °C.

Introduction

Hexaborane(10) and its conjugate base have several potential electron-pair donor sites, but to date this aspect of its chemistry has not been exploited to any great extent.[1] A bridging hydrogen atom in B_6H_{10} may be removed and replaced by electrophilic metal-containing moieties.[2] Thus, complexes containing the metals Mg, Zn, Cd,[3] Pt,[5] and Cu[6] have been prepared. Several years ago proton affinity measurements suggested that B_6H_{10} should act as a base.[7] The species is readily protonated on treatment with HCl, and the basic site was shown to be the direct basal B–B bond.[8] Also, complexes of iron,[9,10] rhodium, iridium, nickel, and platinum,[10,11] in which this bond donates two electrons to the metal, were prepared. Of these systems only the chemistry of $B_6H_{10}Fe(CO)_4$ (I) has been developed, but it has not really been exploited. The species may be deprotonated, and a preliminary report of the properties of its conjugate base, $[B_6H_9Fe(CO)_4]^-$ (II), has appeared.[2a] Derivatives of II $[(CO)_4FeB_7H_{12}]^-$,[12] $(CO)_4FeB_7H_{11}$,[12] and $Cu[P(C_6H_5)_3]_2B_6H_9Fe(CO)_4$,[13] have been prepared, but this represents the extent of any published chemistry for this species. There are very few structural studies available for metalla derivatives of hexaborane(10), and they include the species $Mg(THF)_2(B_6H_9)_2$,[3a] $B_6H_{10}PtCl_2$,[11] and a series of quite complex dimeric molecules in which a $[B_6H_9]^-$ moiety coordinates to two metal atoms.[14,15] Herein we report the crystal and molecular structure for $B_6H_{10}Fe(CO)_4$ along with improved spectral data and also spectral data for its conjugate base, $[B_6H_9Fe(CO)_4]^-$.

[†] To whom correspondence concerning the crystal structure should be addressed.

(1) Barton, L.; Onak, T. P.; Shore, S. G. *Gmelin Handbook of Inorganic Chemistry*; Springer-Verlag: Berlin, 1979; Boron Compounds 20, (New Supplement Series Vol. 54), pp 52–79, and references cited therein.

(2) (a) Shore, S. G.; *Pure App. Chem.* **1977**, *49*, 717. (b) Shore, S. G. In *Boron Hydride Chemistry*; Muetterties, E. L., Ed., Academic Press: New York, 1975; Chapter 3. (c) Gilbert, K. B.; Boocock, S. K.; Shore, S. G. In *Comprehensive Organometallic Chemistry*; Wilkinson, G., Stone, F. G. A., Abel, E. W., Eds.; Pergamon: Oxford, England, 1982; Part 6, Chapter 41, pp 879–945. (d) Kennedy, J. D. *Prog. Inorg. Chem.* **1984**, *32*, 651.

(3) (a) Denton, D. L.; Clayton, W. R.; Mangion, M.; Shore, S. G.; Meyers, E. A. *Inorg. Chem.* **1976**, *15*, 541. (b) Remmel, R. J.; Denton, D. L.; Leach, J. B.; Toft, M. A.; Shore, S. G. *Inorg. Chem.* **1981**, *20*, 1270.

(4) Denton, D. L. Ph.D. Dissertation, The Ohio State University, 1973.

(5) Boocock, S. K.; Greenwood, N. N.; Hails, M. J.; Kennedy, J. D.; McDonald, W. S. *J. Chem. Soc., Dalton Trans.* **1981**, 1415.

(6) (a) Brice, V. T.; Shore, S. G. *J. Chem. Soc., Chem. Commun.* **1970**, 1312. (b) Denton, D. L.; Outterson, G. G.; Barton, L.; Ragaini, J. D.; Shore, S. G. Manuscript in preparation.

(7) Solomon, J. J.; Porter, R. F. *J. Am. Chem. Soc.* **1972**, *94*, 1443.

(8) Johnson, H. D.; Brice, V. T.; Brubaker, G. R.; Shore, S. G. *J. Am. Chem. Soc.* **1972**, *94*, 6711.

(9) Davison, A.; Traficante, D. D.; Wreford, S. S. *J. Chem. Soc., Chem. Commun.* **1972**, 1155.

(10) Davison, A.; Traficante, D. D.; Wreford, S. S. *J. Am. Chem. Soc.* **1974**, *96*, 2802.

(11) Brennan, J. P.; Schaeffer, R.; Davison, A.; Wreford, S. S. *J. Chem. Soc., Chem. Commun.* **1973**, 354.

(12) (a) Hollander, O.; Clayton, W. R.; Shore, S. G. *J. Chem. Soc., Chem. Commun.* **1974**, 604. (b) Mangion, M.; Clayton, W. R.; Hollander, O.; Shore, S. G. *Inorg. Chem.* **1977**, *16*, 2110.

(13) Barton, L.; Srivastava, D. K. *Organometallics* **1991**, *10*, 2892.

(14) (a) Greenwood, N. N.; Hails, M. J.; Kennedy, J. D.; McDonald, W. S. *J. Chem. Soc., Chem. Commun.* **1980**, 37. (b) Greenwood, N. N.; Hails, M. J.; Kennedy, J. D.; McDonald, W. S. *J. Chem. Soc., Dalton Trans.* **1985**, 953. (c) Boocock, S. K.; Greenwood, N. N.; Hails, M. J.; Kennedy, J. D.; McDonald, W. S. *J. Chem. Soc., Dalton Trans.* **1981**, 1415.

0276-7333/93/2312-2017$04.00/0

Table I. 96-MHz ^{11}B NMR Data for I and II

4,5-μ-[Fe(CO)$_4$]-B_6H_{10}^{a} 25 °C	K[$B_6H_9Fe(CO_4)$]^b		
	80 °C	25 °C	–40 °C
–52.5 [d, 1B, B(1), $^1J(^{11}B–^1H)$ = 159 Hz]	–51.0 [d, 1B, B(1), $^1J(^{11}B–^1H)$ = 155 Hz]	–51.5 [d, 1B, B(1), $^1J(^{11}B–^1H)$ = 140 Hz]	–50.5 [d, 1B, B(1), $^1J(^{11}B–^1H)$ = 143 Hz]
2.05 [d, 2B, B(4,5 or 3,6), $^1J(^{11}B–^1H)$ = 138 Hz]			2.01 [s, br, 2B, B(4,5 or 3,6)]
			(4.01)^c
	3.9 [d, 5B, B(2–6), $^1J(^{11}B–^1H)$ = 164 Hz]	ca. 2.31 [s, vbr, 5B, B(2–6)]	
6.79 [d, 2B, B(3,6 or 4,5), $^1J(^{11}B–^1H)$ = 159 Hz]			4.02 [s, br, 2B, B(3,6 or 4,5)]
12.6 [d, 1B, B(2), $^1J(^{11}B–^1H)$ = 148 Hz]			16.2 [s, br, 1 B, B(2)]

^{a} Spectra were recorded in CDCl$_3$; δ values are given in ppm. ^{b} In THF-d_8. ^{c} Weighted average. Uncertainties: δ, ±0.2 ppm; J, ±5 Hz. Abbreviations: s = singlet, d = doublet, br = broad, vbr = very broad.

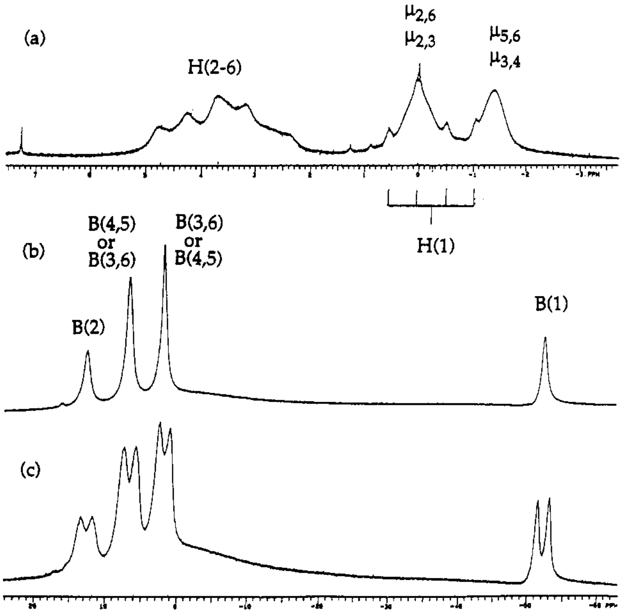

Figure 1. (a) 300-MHz ^{1}H NMR spectrum of I in THF-d_8/$(CD_3)_2O$. (b) 96.3-MHz $^{11}B\{^1H\}$ NMR spectrum of I in CDCl$_3$. (c) ^{11}B NMR spectrum of I in CDCl$_3$.

Experimental Section

Materials. Hexaborane(10) was synthesized using standard literature procedures,[16] and B_5H_9 was obtained from laboratory stock and distilled before use. $Fe_2(CO)_9$ was obtained from Alfa Inorganics and used without further purification. KH, obtained as a mineral oil suspension from Research Organic/Inorganic Chemical Corp., was washed repeatedly with anhydrous pentane on the vacuum line before use until it was a free-flowing white powder. The activity of the powder in reactions with methanol was 85–95%. Dimethyl ether was dried by stirring over LiAlH$_4$ at –78 °C for several days and stored in vacuo. THF and diethyl ether were dried over LiAlH$_4$ followed by Na/benzophenone ketyl and stored over molecular sieves. Pentane was dried over CaH$_2$ followed by Na/benzophenone and stored over molecular sieves. All solvents were reagent grade and were dried and distilled prior to use and stored in Pyrex vessels with Teflon stopcocks.

Apparatus. Standard high-vacuum-line and drybox techniques were employed in this work.[17] NMR spectra were obtained on a Varian XL-300 high-resolution spectrometer operating at 300.1, 96.3, and 76.6 MHz to observe ^{1}H, ^{11}B, and ^{13}C resonances, respectively. ^{11}B chemical shifts were reported in ppm, positive signs denoting shifts to lower field with respect to $(C_2H_5)_2O·BF_3$ reference (0.0 ppm). ^{1}H and ^{13}C chemical shifts were measured relative to Si(CH$_3$)$_4$ and CDCl$_3$, respectively. Boron-decoupled ^{1}H NMR spectra were obtained on a Bruker AM 250-MHz spectrometer. Mass spectra were run as solids at 70 eV on a Varian/Mat 311A spectrometer equipped with a Technivent data system. IR spectra were run as KBr pellets on a Perkin-Elmer 1604 FT-IR spectrometer. Analyses were performed by Schwarzkopf Microanalytical Laboratories.

Synthesis of $B_6H_{10}Fe(CO)_4$. The compound was synthesized by utilizing a slightly modified literature procedure.[9] In a typical reaction, diiron nonacarbonyl (556 mg, 1.53 mmol) and hexaborane(10) (0.4 mL, 3.36 mmol) were stirred in pentane (3 mL) at room temperature overnight. When all the solid had dissolved, the volatiles, which included pentane, excess B_6H_{10}, and Fe(CO)$_5$, were removed under dynamic vacuum at –20 to 0 °C over a period of 2 h. The flask was then warmed to room temperature and the contents were pumped through a trap at –35 °C. $B_6H_{10}Fe(CO)_4$ was obtained as a yellow solid in 60–80% yield. Final purification, including crystal growth, was effected by subliming the $B_6H_{10}Fe(CO)_4$ through a removable U trap maintained at –35 °C (1,2-dichloroethane slush bath) under dynamic vacuum over a period of several hours. The compound is best stored in a refrigerator. Anal. Calcd for $C_4H_{10}B_6FeO_4$: C, 19.68; H, 4.1; B, 27.07. Found: C, 16.73; H, 3.93; B, 25.23. The product was found to be thermally and photolytically unstable, and this accounts for the unsatisfactory elemental analysis. The IR spectrum (KBr) compared well to that reported previously,[10] exhibiting ν_{BH} at 2584, 2553, and 2482 cm^{-1} and ν_{CO} at 2076, 2004, 1975, and 1946 cm^{-1}. ^{11}B and ^{1}H NMR data are given in Tables I and II and displayed in Figure 1. The ^{1}H-decoupled ^{13}C NMR spectrum (CDCl$_3$, 25 °C) gives a singlet at 210 ppm corresponding to 4 CO's. The mass spectrum exhibits the expected B$_6$Fe envelope with a cutoff at m/z(max) 245 attributed to $[^{11}B_6{}^{12}C_4{}^{57}Fe^1H_{10}{}^{16}O_4]^+$. The observed m/z values (relative intensity) for the $B_6H_{10}Fe(CO)_4$ molecular ion cluster were 245 (11.34), 244 (71.74), 243 (100.0), 242 (64.08), 241 (34.13), and 240 (12.55). The calculated m/z data were 245 (3.99), 244 (69.80), 243 (100.0), 242 (61.58), 241 (20.4), and 240 (3.8). Details of the molecular ion envelope along with the calculated one are displayed in Figure 2.

Deprotonation of $Fe(CO)_4B_6H_{10}$ with KH. In the drybox, a 10-mL reaction vessel equipped with a side-arm-attached NMR tube was loaded with 0.05-g sample of $Fe(CO)_4B_6H_{10}$ (0.2 mmol), an excess of KH, and a Teflon-coated magnetic stirring bar. The vessel was fitted with a stopcock adapter and attached to the vacuum while a N$_2$ atmosphere was maintained. After evacuation at –78 °C for 1 h, 1.0 mL of Me$_2$O was condensed in and the reaction mixture was stirred at –78 °C for 2 h. The vessel was frozen, and the H$_2$ evolved was removed. Following H$_2$ evolution, the vessel was warmed to –78 °C and Me$_2$O was pumped away.

---

(15) (a) Ahmad, R.; Crook, J. E.; Greenwood, N. N.; Kennedy, J. D.; McDonald, W. S. *J. Chem. Soc., Chem. Commun.* **1982**, 1019. (b) Beckett, M. A.; Crook, J. E.; Greenwood, N. N.; Kennedy, J. D.; McDonald, W. S. *J. Chem. Soc., Chem. Commun.* **1982**, 552. (c) Beckett, M. A.; Crook, J. E.; Greenwood, N. N.; Kennedy, J. D. *J. Chem. Soc., Chem. Commun.* **1983**, 1228. (d) Ahmad, R.; Crook, J. E.; Greenwood, N. N.; Kennedy, J. D. *J. Chem. Soc., Dalton Trans.* **1986**, 2433. (e) Beckett, M. A.; Crook, J. E.; Greenwood, N. N.; Kennedy, J. D. *J. Chem. Soc., Dalton Trans.* **1986**, 1879.

(16) Remmel, R. J.; Johnson, H. D.; Brice, V. T.; Shore, S. G. *Inorg. Synth.* **1979**, *19*, 247.

(17) Shriver, D. F.; Drezdzon, M. A. *The Manipulation of Air-Sensitive Compounds*; Wiley: New York, 1986.

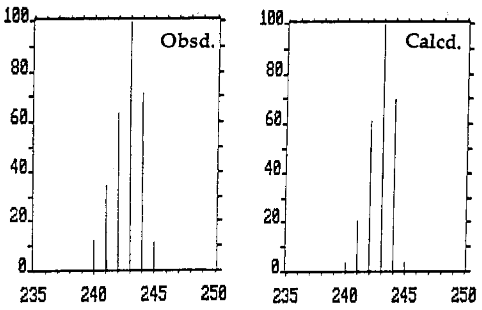

Figure 2. Mass spectral molecular ion profile for 4,5-μ-$[Fe(CO)_4]B_6H_{10}$ (I).

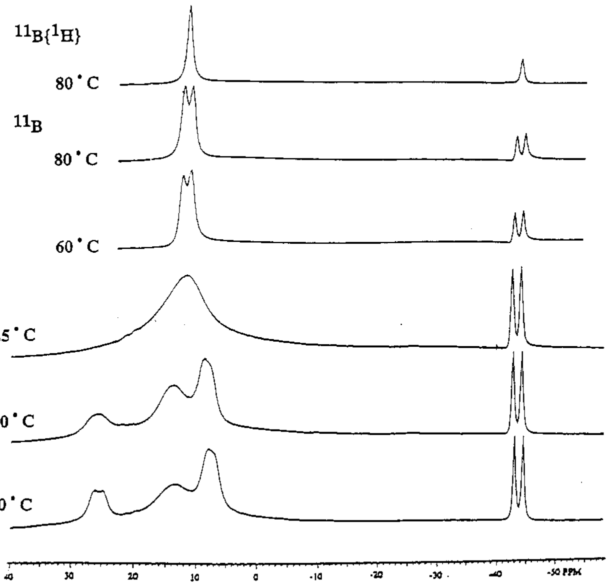

Figure 3. 96.3-MHz variable-temperature ^{11}B NMR spectra of $K[B_6H_9Fe(CO)_4]$ (II) in THF-d_8.

The light brown residue thus obtained was dried at −78 °C for 6 h. THF-d_8 (0.5 mL) was then condensed into the vessel, and the yellowish brown solution was tipped into the attached NMR tube as the whole apparatus was maintained at −78 °C. The tube was sealed with a torch, removed, and stored at −196 °C. NMR spectral data are tabulated in Tables I and II and illustrated in Figures 3 and 4.

X-ray Structure Determination. Crystals of I, suitable for analysis by X-ray diffraction, were obtained by sublimation on the vacuum line as described above. A crystal with the dimensions 0.6 × 0.4 × 0.4 mm was mounted on a glass fiber in a random orientation. Preliminary examination was carried out with Mo Kα radiation using a Siemens R3m/V automated diffractometer equipped with a graphite monochromator. Final cell parameters and the orientation matrix were obtained by least-squares refinement of 30 automatically centered reflections ($30° < 2\Theta < 35°$). Axial photographs of the three axes were taken to confirm the cell lengths and lattice symmetry. An ω scan of representative reflections indicated acceptable crystal quality.

Data were collected at 173 K using the Θ–2Θ scan technique up to a $2\theta_{max}$ value of 65.0°, and the intensities of 4 standard reflections were measured every 50 reflections. No absorption correction was applied to the data. Data reduction, structure solution, and refinement were carried out using the SHELXTL PLUS (VMS)[18] structure solution and refinement package. The structure of I was solved and refined in the orthorhombic space group *Pbca*. The structure was solved by the Patterson method, and the remaining non-hydrogen atoms were located from subsequent difference Fourier maps. Full-matrix least-squares

Table II. 300-MHz Variable-Temperature ^1H NMR Data (δ) for I and II[a]

4,5-μ-$Fe(CO)_4$-B_6H_{10}[b] 25 °C	assignt	$K[B_6H_9Fe(CO)]_4$[c] 80 °C	20 °C	−40 °C	−100 °C	−130 °C	assignt
					−0.470 [s, br, 1H]	−0.335 [s, br, 1H]	$\mu^{3,4}$ or $\mu^{5,6}$
−1.35 [s, br, 2H]	$\mu^{3,4}$ or $\mu^{5,6}$		−1.31 [s, br, 2H]	−1.37 [s, br, 2H]			
						−1.023 [s, br, 1H]	$\mu^{2,6}$ or $\mu^{2,3}$
−0.2 [s, br, 2H]	$\mu^{2,3}$ or $\mu^{2,6}$	−1.66 [s, br, 3H]	(−1.69)[d]			(−1.65)[e]	
			−2.46 [s, br, 1H]	−2.50 [s, br, 1H]	−2.49 [s, br, 2H]		
						−3.60 [s, br, 1H]	$\mu^{5,6}$ or $\mu^{3,4}$
−0.25 [q, br, 1H, $J(^{11}B–^1H)$ = 165 Hz]	H(1)	−1.36 [q, br, 1H $J(^{11}B–^1H)$ = 148 Hz]	−1.38 [q, br, 1H, $J(^{11}B–^1H)$ = 151 Hz]	−1.36 [q, br, 1H, $J(^{11}B–^1H)$ = 143 Hz]	−1.37 [q, br, 1H, *J* poor resolv]	−1.627 [s, br, 1H]	H(1)
				2.87 [s, br, 2H]	2.57 [s, br, 2H]	2.481 [s, br, 2H]	$H^{5,6}$ or $H^{3,6}$
4.73–2.36 [m, br, 5H]	H(2–6)	3.28 (m, br, 5H)	3.25 (m, br, 5H)	(3.35)[c]			
				3.4 [s, br, 2H]	3.2 [s, br, 2H]	3.15 [s, br, 2H]	$H^{3,6}$ or $H^{5,6}$
				3.8 [s, br, 1H]	3.75 [s, br, 1H]	3.81 [s, br, 1H]	H^2

[a] All data are relative to TMS (0.0 ppm). Uncertainties: δ, ±0.2 ppm; *J*, ±5 Hz. Abbreviations: s = singlet, m = multiplet, q = quartet, br = broad. [b] In $CDCl_3$. [c] In THF-d_8/Me_2O. [d] Weighted average. [e] Weighted average of all three resonances.

---

[18] Sheldrick, G. M. Siemens Analytical X-ray Division, Madison, WI, 1990.

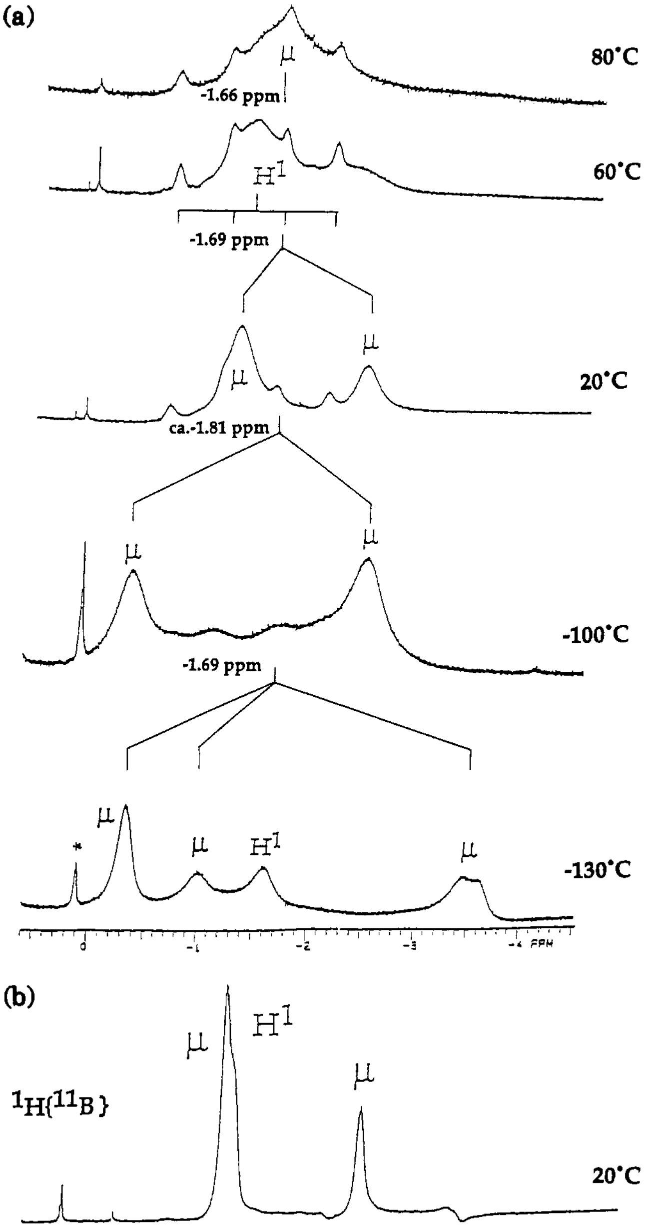

Figure 4. (a) 300-MHz variable-temperature ^1H NMR spectra of II in THF-d_8/$(CD_3)_2O$, in the upfield region of the spectrum. The upper chemical shift given is that for H_μ at 80 °C, and the lower values are the weighted averages of the H_μ signals. (b) $^1H\{^{11}B\}$ spectrum at 20 °C under the same conditions.

refinement was carried out by minimizing the function $w(F_o - F_c)^2$. The hydrogen atoms were located from the difference Fourier maps and were refined isotropically. The non-hydrogen atoms were refined anisotropically to convergence (R = 5.3% and R_w = 7.9% for 2604 observed reflections; $F > 4\sigma(F)$). The final difference Fourier map had a maximum electron density of 0.6 eÅ^{-3}.

Summaries of crystal data, intensity collection parameters, and final structure refinement parameters are presented in Table III. Refined positional parameters for the non-hydrogen atoms are listed in Table IV, and parts a and b of Figure 5 show the projection view and atom-labeling scheme and a view showing the disposition of the $Fe(CO)_4$ moiety relative to an elevation view of the B_6 pyramid, respectively. Tables V and VI list selected bond distances and angles for I.

Results and Discussion

The species $B_6H_{10}Fe(CO)_4$ (I) and $K[Fe(CO)_4B_6H_9]$ (II) are prepared according to eqs 1 and 2.

Table III. Summary of Crystallographic Data for I

empirical formula	$C_4H_{10}B_6FeO_4$
fw	242.8
cryst color, habit	colorless, rectangular
cryst size, mm	0.6 × 0.4 × 0.4
cryst syst	orthorhombic
space group	*Pbca*
unit cell dimens	
a, Å	11.441(3)
b, Å	11.696(4)
c, Å	16.396(3)
V, Å^3	2194.0(10)
Z, molecules/cell	8
D_{calc}, mg m^{-3}	1.470
wavelength, Å	0.710 73
scan type	$2\theta-\theta$
scan speed ω (min–max), deg min^{-1}	3.97–19.53
2θ range deg	3.5–65
T, K	173
abs coeff, mm^{-1}	1.353
abs structure	n/a
no. of rflns collected	5148
no. of ind rflns	3914 (R_{int} = 2.95%)
no. of obs rflns	2604 ($F > 4.0\sigma(F)$)
weighting scheme (w^{-1})	$\sigma^2(F) + 0.0029F^2$
final *R* (obs data), %	5.31
final R_w (obs data), %	7.86
goodness of fit	1.16

Table IV. Atomic Coordinates (×10^4) and Equivalent Isotropic Displacement Coefficients (Å^2 × 10^3) for 4,5-μ-$[Fe(CO)_4]B_6H_{10}$ (I)

atom	*x*	*y*	*z*	*U*(eq)[a]
Fe	2270(1)	1717(1)	208(1)	23(1)
O(1)	3691(2)	3509(2)	–562(1)	34(1)
O(2)	401(2)	1042(2)	–942(1)	39(1)
O(3)	672(2)	3309(2)	1031(2)	36(1)
O(4)	3802(2)	–79(2)	–451(2)	36(1)
C(1)	3139(3)	2829(3)	–256(2)	28(1)
C(2)	1119(3)	1280(3)	–475(2)	28(1)
C(3)	1296(2)	2707(3)	701(2)	27(1)
C(4)	3224(3)	613(3)	–201(2)	28(1)
B(1)	2683(3)	819(3)	2251(2)	28(1)
B(2)	1750(3)	1780(3)	2737(2)	32(1)
B(3)	1174(3)	670(3)	2138(2)	28(1)
B(4)	2071(3)	546(3)	1230(2)	24(1)
B(5)	3264(3)	1523(3)	1355(2)	26(1)
B(6)	3070(3)	2256(3)	2299(2)	31(1)

[a] Equivalent isotropic *U*, defined as one-third of the trace of the orthogonalized U_{ij} tensor.

$$B_6H_{10} + Fe_2(CO)_9 \xrightarrow[25\,°C]{pentane} \underset{I}{Fe(CO)_4B_6H_{10}} + Fe(CO)_5 \quad (1)$$

$$Fe(CO)_4B_6H_{10} + KH \xrightarrow[-78\,°C]{Me_2O} \underset{II}{K[Fe(CO)_4B_6H_9]} + H_2 \quad (2)$$

$Fe(CO)_4B_6H_{10}$ is prepared by stirring B_6H_{10} and $Fe_2(CO)_9$ in pentane and subliming the product mixture through a −35 °C trap. An abundance of yellow rectangular platelike crystals are obtained. The species, which is unstable in air and in the presence of light, did not give a satisfactory elemental analysis, as described in the original report,[9,10] but mass spectral profiles for the parent ion agree very well with those calculated using a program for the calculation of isotopic distributions from molecular formulas.[19] NMR data are given in Tables I and II and are displayed in Figure 1, and the mass spectral ion profile

---

(19) Program for the calculation of isotopic distributions from molecular formulas: Stolz, W.; Korzenioski, R. W. In *Introduction to Organic Spectroscopy*; Lambert, J. B., Shurvell, H. F., Lightner, D. A., Cooks, R. G., Eds.; Macmillan: New York, 1987; pp 401–406.

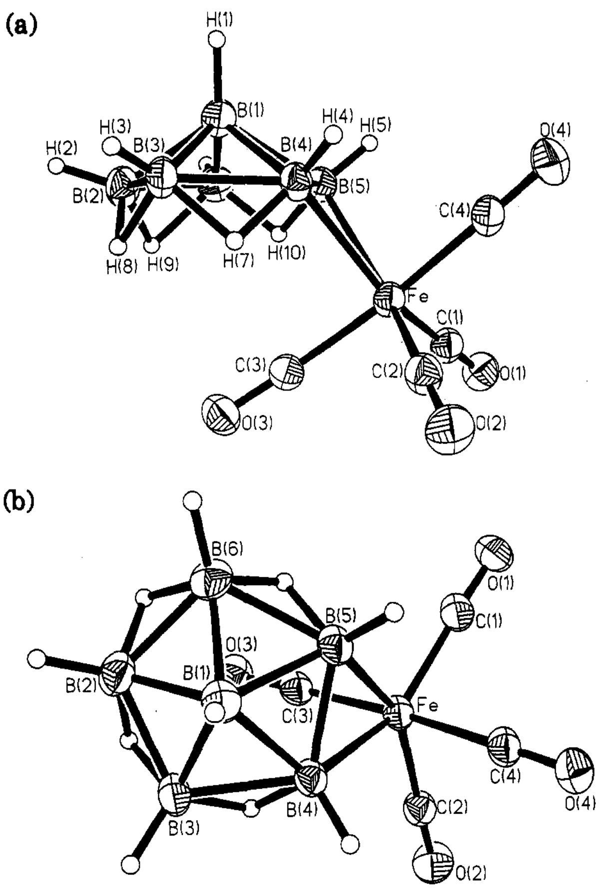

Figure 5. Two views of 4,5-μ-[$Fe(CO)_4$]B_6H_{10} (I): (a) view giving the numbering scheme; (b) view showing the disposition of the $Fe(CO)_4$ moiety relative to the basal plane of the hexaborane cage. The thermal ellipsoids are drawn at the 50% probability level.

data are plotted in Figure 2. A crystal structure determination confirms the structure assumed from previous NMR and analytical data. Two views of the molecular structure are given in parts a and b of Figure 5. The ^{11}B NMR spectra clearly distinguish the four different boron environments, and the ^1H spectrum identifies two groups of equivalent bridging H atoms of δ −1.35 and −0.2 ppm and also the apical H atom at δ −0.25 ppm.

Table V. Selected Bond Lengths (Å) for 4,5-μ-[$Fe(CO)_4$]B_6H_{10} (I)

Fe–C(1)	1.805(3)	Fe–C(2)	1.802(3)
Fe–C(3)	1.799(3)	Fe–C(4)	1.819(3)
Fe–B(4)	2.177(4)	Fe–B(5)	2.183(3)
O(1)–C(1)	1.133(4)	O(2)–C(2)	1.138(4)
O(3)–C(3)	1.139(4)	O(4)–C(4)	1.123(4)
B(1)–B(2)	1.742(5)	B(1)–B(3)	1.746(5)
B(1)–B(4)	1.843(5)	B(1)–B(5)	1.837(5)
B(1)–B(6)	1.739(6)	B(1)–H(1)	1.083(38)
B(2)–B(3)	1.755(5)	B(2)–B(6)	1.762(6)
B(2)–H(2)	1.066(35)	B(2)–H(8)	1.311(37)
B(2)–H(9)	1.308(39)	B(3)–B(4)	1.815(5)
B(3)–H(3)	1.086(40)	B(3)–H(7)	1.337(37)
B(3)–H(8)	1.302(32)	B(4)–B(5)	1.788(5)
B(4)–H(4)	1.094(36)	B(4)–H(7)	1.265(39)
B(5)–B(6)	1.812(5)	B(5)–H(5)	1.073(37)
B(5)–H(10)	1.264(39)	B(6)–H(6)	1.074(38)
B(6)–H(9)	1.373(37)	B(6)–H(10)	1.215(38)

The structure determination confirms that the $Fe(CO_4)$ moiety complexes to the B(4)–B(5) bond of the B_6H_{10} molecule. It also may be considered to replace a proton in $[B_6H_{11}]^+$.[8] The Fe atom is disposed 55.7° below the basal plane B(2–6), a value which is quite similar to analogous dihedral angles in the series of 2,3-μ-pentaboranyl complexes involving the bridging substituents B, Be, Si, Cu, Au, and Sn, which are 52, 56.18, 51.7, 52, 54.2, and 53°, respectively.[20–25] It is essentially identical with the analogous angle[12b] in the related species $[(CO)_4FeB_7H_{12}]^-$, which is 56°. The angles around the Fe atom are consistent with trigonal-bipyramidal geometry. C(1)–Fe–C(2) is 110.3°, and the angles made between the midpoint of B(5)–B(4) to Fe and Fe–C(4) and Fe–C(3) are 122.4 and 127.1°, respectively. The axial bonds Fe–C(3) and Fe–C(4) diverge from the linearity expected for trigonal-bipyramidal geometry by only 6°. The Fe atom lies 0.05 Å above the equatorial plane described by the atoms B(4), B(5), C(1), and C(2). Trigonal-bipyramidal geometry was suggested in the original report of this compound on the basis of Mössbauer spectroscopy.[9] The distances Fe–B(4) and Fe–B(5) are 2.177 and 2.183 Å, respectively, quite similar to those in the related species $[(CO)_4FeB_7H_{12}]^-$, which are 2.218 and 2.196 Å. These distances are longer than the sum of the Pauling covalent radii (1.975 Å), suggesting three-center bonding rather than simple covalent bonding. The distances are also longer than the distances between the Fe atom and the adjacent basal boron atoms in $Cu(Ph_3P)_2B_5H_8Fe(CO)_3$,[26] which are 2.154 and 2.075 Å. Of these last two bonds, the first is a normal covalent one and the second is a B–H–B bridge. The B–B distance for the two-electron bond in the complex which coordinates to the $Fe(CO)_4$ moiety is 1.788 Å, 0.162 Å longer than the analogous bond in uncomplexed B_6H_{10}. The latter distance is 1.626 Å.[27] This opening of the B–B bond on coordination to a metal is observed for other systems. Thus, when Pt inserts into the B(4)–B(5) bond of B_6H_{10}, the new B–B distance is 1.82 Å and in $[(CO)_4FeB_7H_{12}]^-$ it is 1.79 Å.[11,12b] The molecule has a noncrystallographic plane of symmetry passing through B(2), B(1), Fe, and C(4). Deviations from the latter are minor; B(1) lies 0.02 Å above the plane, whereas B(2) and C(4) lie 0.02 Å below the plane. The two sets of equivalent BBB planes differ from each other in the dihedral angle with the basal plane by only 0.1 and 0.4°. A feature of the structure of pentaboranes in which a substituent atom replaces a bridging H atom is that the apical H atom is tilted toward the edge containing the substituent atom.[22,23] In the case of I, the apical H atom is tilted away from the Fe atom. Another feature of the structure is that there appears to be no pattern concerning the bridging H atom bond lengths. The individual lengths are not symmetrically disposed.

$Fe(CO)_4B_6H_{10}$ is deprotonated with KH in THF at −78 °C to afford $K[Fe(CO)_4B_6H_9]$ (II). Although the chemistry of the species has been exploited,[12,13] spectral and dynamic properties of the anion have only been described very briefly in a preliminary report.[2a] The anion is unstable in solution above −30 °C, if there are traces of impurities present, but when very pure it is stable up to 80 °C for

---

(20) Edvenson, G. M.; Gaines, D. F.; Harris, H. A.; Campana, C. F. *Organometallics* **1990**, *9*, 401.

(21) Gaines, D. F.; Coleson, K. M.; Calabrese, J. C. *Inorg. Chem.* **1981**, *20*, 2185.

(22) Calabrese, J. C.; Dahl, L. F. *J. Am. Chem. Soc.* **1971**, *93*, 6042.

(23) Srivastava, D. K.; Rath, N. P.; Barton, L. *Organometallics* **1992**, *11*, 2263.

(24) Greenwood, N. N.; Howard, J. A.; McDonald, W. S. *J. Chem. Soc., Dalton Trans.* **1977**, 37.

(25) Alcock, N. W.; Parkhill, L.; Wallbridge, M. G. H. *Acta Crystallogr.* **1985**, *C41*, 716.

(26) Mangion, M.; Ragaini, J. D.; Schmitkons, T. A.; Shore, S. G. *J. Am. Chem. Soc.* **1979**, *101*, 754.

(27) Huffman, J. C. Ph.D. Thesis, Indiana University, 1974.

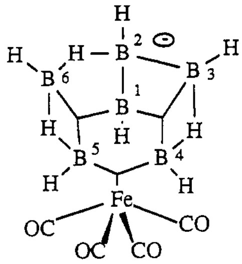

Figure 6. Proposed structure for $[Fe(CO)_4B_6H_9]^-$ (II).

Table VI. Selected Bond Angles (deg) for 4,5-μ-$[Fe(CO)_4]B_6H_{10}$ (I)

C(1)–Fe–C(2)	110.3(1)	C(1)–Fe–C(3)	93.8(1)
C(2)–Fe–C(3)	90.5(1)	C(1)–Fe–C(4)	91.5(1)
C(2)–Fe–C(4)	90.5(1)	C(3)–Fe–C(4)	173.9(1)
C(1)–Fe–B(4)	146.6(1)	C(2)–Fe–B(4)	102.9(1)
C(3)–Fe–B(4)	89.7(1)	C(4)–Fe–B(4)	84.2(1)
C(1)–Fe–B(5)	98.3(1)	C(2)–Fe–B(5)	151.3(1)
C(3)–Fe–B(5)	90.5(1)	C(4)–Fe–B(5)	85.7(1)
B(4)–Fe–B(5)	48.4(1)	Fe–C(1)–O(1)	178.3(3)
Fe–C(2)–O(2)	177.2(3)	Fe–C(3)–O(3)	177.9(3)
Fe–C(4)–O(4)	179.1(3)	B(2)–B(1)–B(3)	60.4(2)
B(2)–B(1)–B(4)	107.1(2)	B(3)–B(1)–B(4)	60.7(2)
B(2)–B(1)–B(5)	107.9(3)	B(3)–B(1)–B(5)	108.4(2)
B(4)–B(1)–B(5)	58.1(2)	B(2)–B(1)–B(6)	60.8(2)
B(3)–B(1)–B(6)	110.7(3)	B(4)–B(1)–B(6)	107.8(2)
B(5)–B(1)–B(6)	60.8(2)	B(2)–B(1)–H(1)	123.0(20)
B(3)–B(1)–H(1)	119.3(21)	B(4)–B(1)–H(1)	121.2(20)
B(5)–B(1)–H(1)	122.0(21)	B(6)–B(1)–H(1)	121.8(20)
B(1)–B(2)–B(3)	59.9(2)	B(1)–B(2)–B(6)	59.5(2)
B(3)–B(2)–B(6)	109.2(3)	B(1)–B(2)–H(2)	128.3(17)
B(3)–B(2)–H(2)	124.1(17)	B(6)–B(2)–H(2)	120.8(18)
B(1)–B(2)–H(8)	102.7(15)	B(3)–B(2)–H(8)	47.6(14)
B(6)–B(2)–H(8)	122.0(15)	H(2)–B(2)–H(8)	112.8(24)
B(1)–B(2)–H(9)	106.8(17)	B(3)–B(2)–H(9)	126.3(17)
B(6)–B(2)–H(9)	50.5(16)	H(2)–B(2)–H(9)	105.0(24)
H(8)–B(2)–H(9)	96.8(21)	B(1)–B(3)–B(2)	59.7(2)
B(1)–B(3)–B(4)	62.3(2)	B(2)–B(3)–B(4)	107.8(2)
B(1)–B(3)–H(3)	128.1(21)	B(2)–B(3)–H(3)	121.1(20)
B(4)–B(3)–H(3)	127.4(20)	B(1)–B(3)–H(7)	103.0(17)
B(2)–B(3)–H(7)	120.0(17)	B(4)–B(3)–H(7)	44.2(17)
H(3)–B(3)–H(7)	113.8(26)	B(1)–B(3)–H(8)	102.9(16)
B(2)–B(3)–H(8)	48.0(16)	B(4)–B(3)–H(8)	116.4(16)
H(3)–B(3)–H(8)	110.4(26)	H(7)–B(3)–H(8)	92.5(23)
Fe–B(4)–B(1)	123.5(2)	Fe–B(4)–B(3)	129.8(2)
B(1)–B(4)–B(3)	57.0(2)	Fe–B(4)–B(5)	66.0(2)
B(1)–B(4)–B(5)	60.8(2)	B(3)–B(4)–B(5)	107.6(2)
Fe–B(4)–H(4)	110.8(19)	B(1)–B(4)–H(4)	115.0(19)
B(3)–B(4)–H(4)	111.1(19)	B(5)–B(4)–H(4)	126.4(17)
Fe–B(4)–H(7)	92.6(17)	B(1)–B(4)–H(7)	101.0(17)
B(3)–B(4)–H(7)	47.4(17)	B(5)–B(4)–H(7)	123.5(18)
H(4)–B(4)–H(7)	109.9(24)	Fe–B(5)–B(1)	123.4(2)
Fe–B(5)–B(4)	65.6(2)	B(1)–B(5)–B(4)	61.1(2)
Fe–B(5)–B(6)	128.7(2)	B(1)–B(5)–B(6)	56.9(2)
B(4)–B(5)–B(6)	107.0(2)	Fe–B(5)–H(5)	110.9(19)
B(1)–B(5)–H(5)	112.9(20)	B(4)–B(5)–H(5)	123.0(21)
B(6)–B(5)–H(5)	113.8(20)	Fe–B(5)–H(10)	95.5(17)
B(1)–B(5)–H(10)	95.6(18)	B(4)–B(5)–H(10)	120.6(17)
B(6)–B(5)–H(10)	42.0(17)	H(5)–B(5)–H(10)	116.4(27)
B(1)–B(6)–B(2)	59.7(2)	B(1)–B(6)–B(5)	62.3(2)
B(2)–B(6)–B(5)	108.1(3)	B(1)–B(6)–H(6)	129.7(19)
B(2)–B(6)–H(6)	121.0(21)	B(5)–B(6)–H(6)	127.7(21)
B(1)–B(6)–H(9)	103.9(16)	B(2)–B(6)–H(9)	47.4(16)
B(5)–B(6)–H(9)	121.1(17)	H(6)–B(6)–H(9)	105.5(26)
B(1)–B(6)–H(10)	102.6(19)	B(2)–B(6)–H(10)	119.6(18)
B(5)–B(6)–H(10)	44.1(19)	H(6)–B(6)–H(10)	113.6(27)
H(9)–B(6)–H(10)	96.1(25)	B(3)–H(7)–B(4)	88.4(23)
B(2)–H(8)–B(3)	84.4(20)	B(2)–H(9)–B(6)	82.1(22)

several minutes. NMR spectral data for II are listed in Tables I and II. The proposed static structure of II is given in Figure 6, and ^{11}B NMR spectra at various temperatures are given in Figure 3. At room temperature the spectrum exhibits a broad featureless resonance centered at 2.31 ppm, assigned to the five basal boron atoms, and a well-resolved doublet upfield at −51.5 ppm assigned to the apical boron. If the sample is cooled to −40 °C, the broad resonance splits into three resonances in the area ratio 1:2:2 at 16.2, 4.02, and −2.1 ppm, respectively, resembling the spectrum of $Fe(CO)_4B_6H_{10}$ and suggesting the presence of a plane of symmetry. At lower temperatures the spectra broaden substantially. When the sample is warmed above room temperature, the basal resonance sharpens so that at 80 °C a sharp doublet of area ratio 5 is observed at 3.9 ppm, which compared well with the weighted average of the signals at −40 °C of 4.01 ppm. The spectra suggest fluxional motion at high temperaures which renders all the basal B atoms equivalent on the NMR time scale. It has been established that pyramidal boranes such as B_6H_{10}, which have an unbridged basal B–B bond, are fluxional because the bridging H atoms were able to move in and out of the site provided by the B–B bond.[28,29]

The proton NMR spectrum of $[Fe(CO)_4B_6H_9]^-$ at room temperature exhibits a single broad resonance at 3.28 ppm for the terminal hydrogens bonded to the basal boron atoms. These begin to split into three resonances around −10 °C so that, at −40 °C, three resonances in the area ratio 2:2:1 are observed at 2.87, 3.4, and 3.8 ppm, respectively. These resonances are essentially unchanged down to −130 °C. The proton spectra in the upfield region of the spectrum reveal additional information and allow us to make suggestions about the fluxional processes. The data are given in Table II. At the highest temperature at which we recorded spectra, 80 °C, a single resonance is observed for the bridging H atoms at −1.66 ppm and a single resonance is seen for the hydrogen on the apical boron atom, H(1). The latter is observed as a 1:1:1:1 quartet which on ^{11}B decoupling gives a singlet at −1.36 ppm. The observations on the bridge hydrogen resonances imply that they are equivalent on the proton and boron-11 NMR time scale at 80 °C. As the temperature is lowered, the single resonance begins to split into two resonances of area ratio 2:1. This process appears to be complete just below 25 °C when two distinct resonances of area ratio 2:1 at −1.31 and −2.46 ppm, respectively, are observed. The weighted average of these two resonances is −1.69 ppm, comparing well with the value at 80 °C. These two resonances are at their sharpest in the region where the basal boron atom resonance in the ^{11}B spectrum begins to split into three resonances, that is at about −10 °C. As the temperature is lowered, the resonance at lower field begins to broaden and eventually splits such that at −100 °C two resonances are observed in approximately 1:2 ratio. Although these resonances are still somewhat coalesced, the new weighted average of the signals is still in reasonable agreement with the value at room temperature, i.e. −1.81 ppm. As the temperature is lowered further, the lower field bridging resonance splits such that at −130 °C three resonances assigned to the bridging H atoms are seen at −0.34, −1.03, and −3.60 ppm. The weighted average of these three is −1.65 ppm. The ^1H spectra between 80 and −130 °C are displayed in Figure 4.

Variable-temperature carbon-13 NMR spectra of K-$[B_6H_9Fe(CO)_4]$ in dimethyl ether were obtained in an effort to understand the behavior of the carbonyl ligands in

---

(28) Brice, V. T.; Johnson, H. D.; Shore, S. G. *J. Am. Chem. Soc.* **1973**, *95*, 6629.

(29) Rush, P. K.; Barton, L. *Polyhedron* **1985**, *4*, 1741.

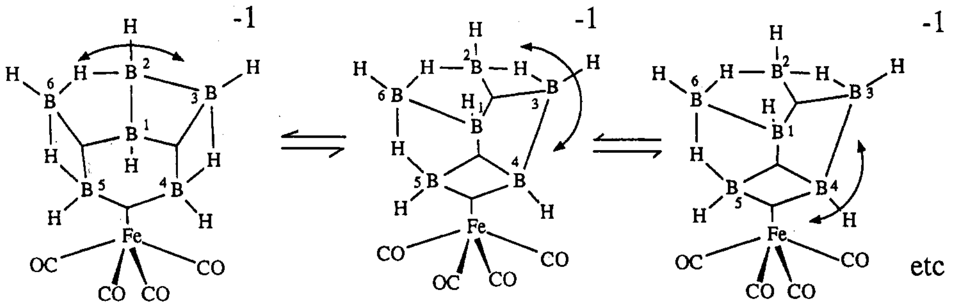

Figure 7. Possible mechanism for the fluxional motion of the H_μ atoms and the $Fe(CO)_4$ moeity in $[Fe(CO)_4B_6H_9]^-$ (II).

solution. The results reveal that the carbonyl groups in the $Fe(CO)_4$ moiety are fluxional. At −135 °C, two equal-area peaks are observed at δ 219.2 and 218.8 presumably due to the axial and equatorial carbonyl resonances. Although the two axial carbonyl ligands are not equivalent, they cannot be resolved and are presumably coincidental. As the solution is warmed slowly, broadening of the peaks occurs and coalescence into a single broad resonance (δ 218.9) is observed at −115 °C. On further warming, the peaks begin to sharpen and a single sharp resonance (δ 218.8) is observed in the temperature range −88 to 0 °C. This observation suggests that apparently a dynamic process, presumably intramolecular carbonyl exchange, is occurring which renders all the carbonyls equivalent on the NMR time scale in the temperature range −115 to 0 °C. However, below −115 °C, carbonyl migration appears to be quenched, leading to two sets of carbonyl environments. Using the dynamic ^{13}C NMR data, estimates of the energy barriers for the exchange processes may be made. Assuming a coalescence temperature of −115 °C (158 K) and $\delta\nu$ = 28.3 Hz, the free energy of activation for the rotation at the coalescence temperature is estimated to be very low, on the order of 1 kcal mol^{-1}.[30]

At the highest temperatures, the observation of only one B environment suggests that there is dynamic motion involving the bridging H atoms, the $Fe(CO)_4$ moiety, and the borane cage. A possible mechanism would involve the $H\mu$ atoms moving in and out of the B–B bond. This could also occur for the Fe moiety, but since it is so large, perhaps the cage moves relative to the metal. Possible processes are suggested in Figure 7. Such motion was proposed previously in the case of the species $(THF)_2Mg(B_6H_9)_2$[3a] and $(THF)_2Mg(2\text{-}CH_3B_6H_8)_2$.[3b] The observation of a single resonance for $H\mu$ suggests that the $Fe(CO)_4$ moiety moves by a 1,3-shift, since a 1,2-shift should result in one of the H atoms always being flanked by two others, resulting in two resonances in a 2:1 ratio. A possible mechanism for the 1,3-shift would involve a rocking motion of the borane cage on the Fe atom, as indicated in Figure 8. This would remove the restriction of the relative positions of the three $H\mu$ atoms and allow all three to be equivalent on the NMR time scale if the motions illustrated in Figures 7 and 8 occur simultaneously or concurrently. An alternative to this involves a dissociative mechanism involving equilibrium between $[B_6H_9]^-$ and $Fe(CO)_4$ in the THF solvent: $[B_6H_9Fe(CO)_4]^- + THF = [B_6H_9]^- + THF{\cdot}Fe(CO)_4$. We cannot rule this out, but we do not favor it. The free borane anion is very unstable and thus should decompose, and the $Fe(CO)_4$ moiety should eventually afford $Fe_3(CO)_{12}$. We see no evidence of the latter species.

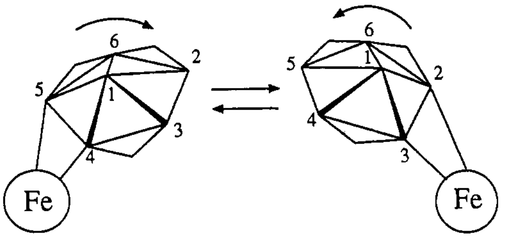

Figure 8. Possible mechanisms for a 1,3-shift of the $Fe(CO)_4$ moiety relative to the borane cage in $[Fe(CO)_4B_6H_9]^-$ (II).

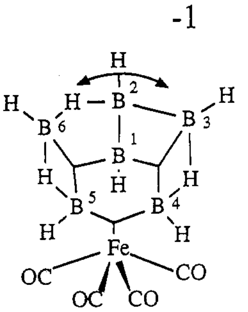

Figure 9. Proposed partially quenched motion of the bridging H atoms in $[Fe(CO)_4B_6H_9]^-$ (II).

As the temperature is lowered, the motion of the cage relative to the Fe moiety slows down. Thus, below room temperature three resonances are observed for the basal borons and in the proton spectrum two resonances of area ratio 2:1 are observed for the bridging hydrogen atoms. In this case the three $H\mu$ atoms are moving freely between the four available sites B(2)–B(3), B(3)–B(4), B(5)–B(6), and B(6)–B(2). As the temperature is lowered further, at −100 °C the three H_μ atoms are observed as two resonances in a 1:2 area ratio. Apparently the system is further quenched partially such that only one atom moves between sites B(2)–B(3) and B(2)–B(6), and the other two bridge hydrogens are fixed in positions adjacent to the $Fe(CO)_4$ moiety. This latter phenomenon has been proposed for $(THF)_2Mg(B_6H_9)_2$,[3b] $[2\text{-}CH_3B_6H_9]$,[3b] and $2,3\text{-}\mu\text{-}(SnPh_3)B_6H_9$.[31] This is illustrated in Figure 9. As the temperature is lowered further, at −130 °C all three $H\mu$ atoms are observed. The system is completely quenched, and as indicated in Figure 4, three resonances are observed. The weighted average of the three observed resonances is δ −1.65, agreeing quite well with the weighted averages of the resonances observed at higher temperatures and with the averaged resonance seen at 80 °C.

---

[30] Based on use of the approximate equation $\Delta G^{\ddagger} = \{19.14T_c[9.97 + \log(T_c/\delta\nu)]\}$ in J mol^{-1}, where $\delta\nu$ is the difference between resonance frequencies in Hz, T_c is the coalescence temperature, and $\Delta G^{\ddagger}$ is the energy barrier in J mol^{-1}. See: Kost, D.; Carlson, E. H.; Raban, M. *J. Chem. Soc. D* 1971, 656. Gunther, H. *NMR Spectroscopy: An Introduction*; Wiley: New York, 1980; pp 242–244.

[31] Srivastava, D. K.; Barton, L. Submitted for publication in *Organometallics*.

Conclusions

We have structurally characterized 4,5-μ-[Fe(CO)$_4$]B_6H_{10}, only the third simple B_6H_{10} derivative for which a crystal structure determination has been possible. The conjugate base, $[Fe(CO)_4]B_6H_9]^-$, has some unusual and novel dynamic properties for which variable-temperature NMR data provide some information on the possible processes occurring. Fluxional motion of both the bridging H atoms in and out of the basal B–B bond and also motion of the cage with respect to the $Fe(CO)_4$ moiety are suggested in order to explain the observations. Prior to complete quenching of the motion, the system is partially quenched. Effectively, two bridge H atoms are fixed adjacent to the B–B bond to which the $Fe(CO)_4$ moiety is coordinated, while the third H_μ atom moves between the two available sites. We expect that these observations will assist in the interpretation of the spectra of other hexaborane(10) species and related derivatives and we intend to report some such results in the near future.[31]

Acknowledgment. We acknowledge the support of the Monsanto Co. and the Missouri Research Assistance Act in the form of a postdoctoral fellowship to D.K.S., to UM—St. Louis for an IRQ Award, and the National Science Foundation for the grant for the NMR spectrometer (No. CHE-8506671). S.G.S. acknowledges partial support of this work through grants from the National Science Foundation.

Supplementary Material Available: Tables of anisotropic thermal parameters and coordinates for the hydrogen atoms for I (2 pages). Ordering information is given on any current masthead page.

OM9207370